

Three-body molecular states of the LiH_2^+ system in the Born–Oppenheimer approximation

Juan M. Randazzo¹  | Antonio Aguilar-Navarro²

¹Departamento de Interacción de la Radiación con la Materia, Centro Atómico Bariloche and CONICET, 8400 San Carlos de Bariloche, Río Negro, Argentina

²Departamento de Química Física, Universidad de Barcelona, 08028, Barcelona, España

Correspondence

Juan Martín Randazzo, Centro Atómico Bariloche, Departamento de Interacción de la Radiación con la Materia, Centro Atómico Bariloche and CONICET, Av. Bustillo Km 9500., San Carlos de Bariloche, Río Negro, Argentina.
Email: randazzo@cab.cnea.gov.ar

Funding information

Universidad Nacional de Cuyo, Project Number: 06/C480; FONCYT, Grant/Award Number: PICT-2014-1400; CONICET

Abstract

In this work, we present a quantum mechanical treatment of the three-body LiH_2^+ molecular system in the Born–Oppenheimer (BO) approximation, where the nuclei dynamics is evaluated over the potential energy surfaces (PES) induced by the electronic states. The PES corresponding to the two lowest electronic levels are the ones described by Martinazzo et al. (Chem. Phys. 2003, 287, 335), and are used to write the three-body Schrödinger equation of the three atomic system. We use the generalized Sturmian functions method to expand the wave functions in each (distinguishable) pair of relative coordinates or Jacobi pairs, and analyze the convergence differences between the series. A partial-wave decomposition of the potential is proposed to simplify the Hamiltonian matrix element calculation. Bound states are considered for the ground and first excited electronic PES, the spreading of energies after sudden electronic transitions studied, and the break-up probability induced by the sudden change of the PES evidenced.

KEYWORDS

Born–Oppenheimer, bound states, potential energy surface, reactive scattering, Sturmian functions

1 | INTRODUCTION

In the last decades there have been significant advances in the studies of the LiH_2^+ and related bound and collisional systems, in the context of the physical chemistry of the early universe.^[1–4] According to S. Lepp et al.,^[5] LiH and LiH^+ may act as coolant, and then their abundances become deterministic for the clouds to collapse to form stars. The formation of these diatomic molecules is doubt principally by the radiative reactions of the form:



while a subsequent collision with hydrogen (or deuterium) can produce Li^+ again:



Substantial progress in the study of these and similar reactions became possible thanks to the development of potential energy surfaces (PES)^[6–8] which describe the interaction between the three atomic nuclei. In this approximation, the electronic motion is decoupled from the nuclei dynamics, which is supposed to be much more slowly because of the mass differences. For each fixed space configuration of the three Coulomb fields, a many-electron state is evaluated by means of a multi reference valence bond approach within a spin-coupled formulation.^[9] From the energy values, a potential energy surface which depends on the three relative atomic coordinates is obtained, and from it, many properties of the system's reactions can be analyzed, such as possible reactive paths and reaction potentials.

To complete the description of the system one has to determine the dynamics of the three atoms interacting through the potential energy surface. At this stage a further approach is sometimes realized by considering classical trajectories, followed by an ad hoc mapping of the final classical states into the quantum channels, to define the cross sections. This is justified by the fact that heavy particles have a dense spectrum in energy and angular momentum, which can be considered to be continuous, together with the fact that the spread of the wave packets is small, making the quantum dynamics similar to classical motion in some cases. Because of the dense discretization of the angular momentum, the quantum treatment

is very difficult from the numerical point of view. It can be applied only to some particular three-body systems, while s-wave approaches have been considered for four body problems.^[10]

In the last years, we have developed a Generalized Sturmian Functions (GSF) approach to study three-body systems associated to atomic and collisional problems.^[11] Basically, it allows us to deal with the bound states of two-electron atoms,^[12] as well as the two electron continuum associated to single and double ionization by electron, ion or photon impact.^[13,14] Recently, we have applied to determine the collective dynamics of a confined proton-electron pair without resorting to the BO approximation.^[15] The method is based on the Sturmian expansion in two of the three interparticle distances or Jacobi pairs (tested here for the first time), which is able to adequately impose a variety of asymptotic conditions such as the stationary ones associated to bound states or the outgoing (incoming) wave behavior corresponding to the scattering states. Due to the masses of the particles involved in these systems, for low energies the partial wave expansion converges with a relatively low number of terms.

It is the aim of this work to test this methodology at the regimes associated to molecular bound states. We will investigate solutions to a three-body Schrödinger equation for the atomic motion of the LiH_2^+ system. We will explore different coordinate systems which can be used to describe the system and write the Schrödinger equation: two relative coordinates or Jacobi pairs. These can be chosen in different ways, and each of them gives a better representation of some of the asymptotic interactions. We will express the wave function as a combination of Sturmian functions for the radial coordinates of the different possible vectors, and bispherical harmonics for the angular ones, which will allow us to write eigenfunctions of the total angular momentum quantum number and its projection on a given axes. In the matrix representation of the Hamiltonian, the kinetic energy and overlaps correspond to analytical or one-dimensional integrals. Special care must be taken when dealing with the potential, which comes from a numerical subroutine and depends on the three relative coordinates. A proper numerical partial-wave decomposition is performed to decouple the integrals. The matrix representation of the Hamiltonian followed with the Galerkin method will allow us to find the eigenenergies and eigenstates.

The article is organized as follows. In section 2, the expressions for the three-body molecular Hamiltonian are given in terms of any couple of relative coordinates or Jacobi pairs. We propose a partial-wave expansion of the three body potential, to reduce to the minimum the dimension of the integrals of the Hamiltonian matrix elements. The expansion of the three-body molecular states in terms of the Sturmian basis functions which includes potentials optimized to each coordinate system is proposed. In section 3 results are presented, including a convergence analysis as a function of the radial coordinates and the partial wave order. The harmonic generation produced by a sudden electronic transition and its effect on the atomic ground state associated to the excited state electronic PES are also studied. Finally, in section 4, some conclusions are drawn. We use atomic units throughout.

2 | METHODOLOGY

In this section we describe how the Schrödinger equation for the three-body LiH_2^+ molecular system is solved by means of the generalized Sturmian method. The technique applies for a general three-body system with masses m_i ($i = 1, 2, 3$) which interact through a given potential $U(r_{12}, r_{13}, r_{23})$, which depends only on the relative particle's distances. Below we describe the procedure, either when we use relative or Jacobi pairs coordinates.

2.1 | Relative coordinates

In terms of the relative coordinates (RC) the three-body Schrödinger equation can be written as:

$$\left[-\frac{1}{2\mu_{13}} \nabla_{r_{13}}^2 - \frac{1}{2\mu_{23}} \nabla_{r_{23}}^2 - \frac{1}{m_3} \nabla_{r_{13}} \cdot \nabla_{r_{23}} + U(r_{12}, r_{13}, r_{23}) - E \right] \Psi(\mathbf{r}_{13}, \mathbf{r}_{23}) = 0, \quad (3)$$

where $U(r_{12}, r_{13}, r_{23})$ is the interaction potential which depends on the magnitude of the three RC $\mathbf{r}_{13} = \mathbf{r}_1 - \mathbf{r}_3$, $\mathbf{r}_{23} = \mathbf{r}_2 - \mathbf{r}_3$, and $\mathbf{r}_{12} = \mathbf{r}_1 - \mathbf{r}_2$, where \mathbf{r}_i ($i = 1, 2, 3$) is the vector which locates the particle i with mass m_i respect to some inertial reference frame, while $\mu_{j3} = m_j m_3 / (m_j + m_3)$ ($j = 1, 2$) are the reduced masses. Note that permutation of the labels ($i = 1, 2, 3$) gives different expressions for the equation which describes the same dynamics. Approximate solutions given by numerical methods will present differences, each of which could be adequate to describe a particular physical process or asymptotic region.

In the next sections we will specify coordinates for the LiH_2^+ system, while U would correspond to the potential energy surfaces (PES) of the triatomic system in the approach given by Martinazzo et al.^[7] As previously mentioned, there is more than one way for the coordinate to be assigned the indexes to the particles, each of them implying a different numerical treatment of the interaction and dynamics. In the following we will suppress the number 3 in the subindex of the vector so that $\mathbf{r}_1 \equiv \mathbf{r}_{13}$ and $\mathbf{r}_2 \equiv \mathbf{r}_{23}$.

We propose the following solution to Equation 3:

$$\Psi^{L,M}(\mathbf{r}_1, \mathbf{r}_2) = \sum_{\nu} a_{\nu}^{L,M} \Phi_{\nu}^{L,M}(\mathbf{r}_1, \mathbf{r}_2) = \sum_{l_1, l_2} R_{l_1, l_2}^{L,M}(\mathbf{r}_1, \mathbf{r}_2) \mathcal{Y}_{l_1, l_2}^{L,M}(\hat{\mathbf{r}}_1, \hat{\mathbf{r}}_2), \quad (4)$$

where

$$R_{l_1, l_2}^{L,M}(\mathbf{r}_1, \mathbf{r}_2) = \sum_{n_1, n_2} a_{\nu}^{L,M} \frac{S_{n_1}(r_1) S_{n_2}(r_2)}{r_1 r_2}. \quad (5)$$

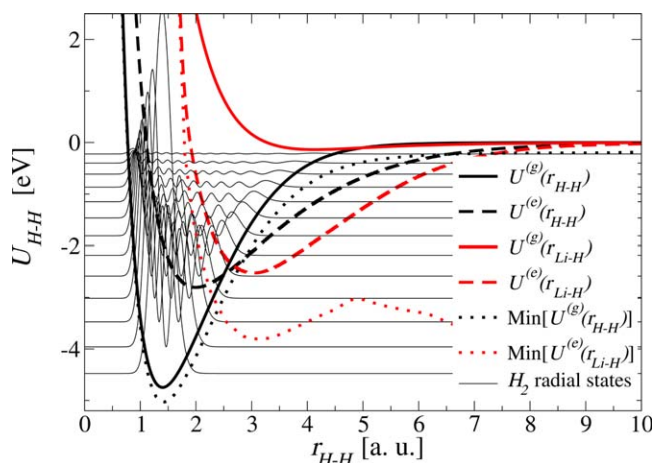


FIGURE 1 Two body PES for the H–H system, which are obtained at the asymptotic limits of U^g . The minimum potentials are used in the sturmian equation (see text). Superposed to the potentials we plot some of the radial “s” states for each system

and $v = \{l_1, l_2, n_1, n_2\}$ stands for the set of single particle radial and angular quantum numbers. $\mathcal{Y}_{l_1, l_2}^{L, M}$ are the bi-spherical harmonics, eigenfunctions of the total angular momentum operator projection over the \hat{z} axis with respective quantum numbers L and M . Since the potential depends only on the inter particle distances (and note their angles), the total angular momentum is a constant of motion.^[16]

The functions S_n correspond to the generalized Sturmian functions (GSF) basis,^[11] in this case chosen to satisfy the equations:

$$\left[-\frac{1}{2\mu_{i3}} \frac{d^2}{dr_i^2} + U_i(r_i) - E_i + \beta_{n_i} V_i(r_i) \right] S_{n_i}(r_i) = 0 \quad (i=1, 2) \quad (6)$$

where E is an externally fixed parameter and β is the eigenvalue associated to the *generating* potential V . As in previous contributions,^[11] we will refer to U as the *auxiliary* potential, and it is introduced to provide the basis with some information about the physical system. In atomic calculations, we choose U as the asymptotic part of the three-body potential, which in this case it would correspond, for example, to $U_1(r_1) = U^{(j)}(r_1, \infty, \infty)$ and $U_2(r_2) = U^{(j)}(\infty, r_2, \infty)$, where $j = g, e$, respectively, stands for the ground and first excited electronic PES. These potentials correspond to the H–H and Li–H interactions when the Li and one of the hydrogen atoms is far apart respectively. From them we can obtain the asymptotic two body states as it is shown in Figures 1 and 2 for some $l = 0$ radial states.

For the problem considered here however, this proposal do not represent the dynamics when the third particle becomes closer, since the typical repulsive barrier of the (two body) interatomic potential could be diminished by the presence of the third one (the potential cannot be separated in three asymptotic parts). If we force the basis with a repulsive barrier we would need a huge number of basis elements to allow the probability to be different from zero when the third particle becomes close. Instead, we propose:

$$U_1(r_1) = \text{Min}[U^{(j)}(r_1, r_2, r_3)] \{0 \leq r_2 \leq \infty; |r_1 - r_2| \leq r_3 \leq r_1 + r_2\}, \quad (7)$$

that is, the minimum value that the potential can take for any value of the other two inter-particle coordinates, and an equivalent definition for $U_2(r_2)$.

Equation 6 is defined to impose the boundary conditions associated to the physical problem on the functions S .^[12] They are solved numerically, using a finite-difference scheme and specially adapted diagonalization procedures to avoid instabilities.^[17] The particular values of E_i and $V(r_i)$ ($i = 1, 2$) used for the present calculations will be given later.

According to Martinazzo et al.,^[7] the difference between the ground and first excited electronic state PES corresponds to the different ways in which the electrons associate to the atoms while they move away from each other in the LiH_2^+ ionic system. The ground state PES correspond to the electronic state at which the H_2 system stay neutral when they move apart from the Li^+ ion. That means that at the asymptotic regions one finds the $\text{LiH}^+ + \text{H}$ or $\text{Li}^+ + \text{H} + \text{H}$ systems, that is the positive charge is always accompanying the Li atom. In the first excited state, instead, one of the hydrogen atoms stays ionized in the asymptotic regions: $\text{LiH} + \text{H}^+$ and $\text{Li} + \text{H} + \text{H}^+$. Having two identical H atoms has two important implications. First, the ground and first excited PES are symmetric under the interchange of H atom coordinates. Second, the first excited electronic state PES is degenerate with the second one in the asymptotic region, and in the inner region the difference in energy is much smaller than the difference between the ground and the first excited electronic PES. This description will explain the asymmetries of the partial wave terms of the potential and states corresponding to the first excited electronic state PES. A more detailed physical description of the surfaces can be read at Ref. 7.

Replacement of expression (4) into Equation 3, making use of Equation 6, and projecting each of the basis elements $\Phi_{\nu}^{L, M}$ onto the left, we arrive at a generalized eigenvalue problem for the coefficients $a_{\nu}^{L, M}$, whose solutions are the energies and bound (and some stationary pseudo-continuum) states of the system. The matrix equation reads:

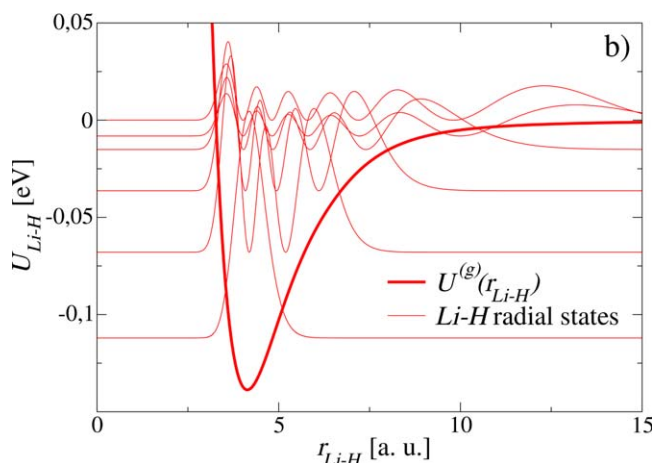


FIGURE 2 Same as Figure 1, in this case for the Li–H system

$$\mathbf{H}\mathbf{a} = \hat{E}\mathbf{O}\mathbf{a} \quad (8)$$

where \mathbf{a} is the vector composed by the coefficients $a_v^{L,M}$, E is the eigenvalue which is related to the energy through $\hat{E} = E - E_1 - E_2$, and $\mathbf{H} = \mathbf{G} + \mathbf{h}_1 + \mathbf{h}_2 + \mathbf{U}$, where:

$$\begin{aligned} [\mathbf{G}]_{v,v} &= \left\langle \Phi_v^{L,M} \left| -\frac{1}{m_3} \nabla_{r_1} \cdot \nabla_{r_2} \right| \Phi_v^{L,M} \right\rangle, \\ [\mathbf{U}]_{v,v} &= \left\langle \Phi_v^{L,M} \left| \tilde{U}(r_{12}, r_1, r_2) \right| \Phi_v^{L,M} \right\rangle, \\ [\mathbf{O}_{v,v}] &= \left\langle \Phi_v^{L,M} \left| \Phi_v^{L,M} \right\rangle, \\ [\mathbf{h}_1]_{v,v} &= \left\langle \Phi_v^{L,M} \left| -\beta_{n_1} V(r_1) + \frac{l_1(l_1+1)}{2\mu_{13}r_1^2} \right| \Phi_v^{L,M} \right\rangle \end{aligned} \quad (9)$$

and

$$[\mathbf{h}_2]_{v,v} = \left\langle \Phi_v^{L,M} \left| -\beta_{n_2} V(r_2) + \frac{l_2(l_2+1)}{2\mu_{23}r_2^2} \right| \Phi_v^{L,M} \right\rangle,$$

where $\tilde{U}(r_{12}, r_1, r_2) = U(r_{12}, r_1, r_2) - U_1(r_1) - U_2(r_2)$. All the matrix elements which does not involve \tilde{U} are separable in spherical coordinates, where the angular integrals can be evaluated exactly, while Gauss–Legendre quadrature is employed for the radial ones. The elements $[\mathbf{U}]_{v,v}$ involve integration on coordinates r_1 , r_2 , and r_{12} , whose value comes from a Fortran Routine, that is, it does not have a simple analytical expression. To deal with these matrix elements, we define a partial wave series:

$$\tilde{U}(r_{12}, r_1, r_2) = \sum_{l=0}^{\infty} \tilde{U}_l(r_1, r_2) P_l(\cos \theta_{12}) \quad (10)$$

where θ_{12} is the angle between \hat{r}_1 and \hat{r}_2 , P_l is the Legendre polynomial, and:

$$\tilde{U}_l(r_1, r_2) = \frac{2l+1}{2} \int_{-1}^1 \tilde{u}(r_1, r_2, x) P_l(x) dx. \quad (11)$$

where $\tilde{u}(r_1, r_2, x) = \tilde{U}((r_1^2 + r_2^2 - r_1 r_2 x)^{1/2}, r_1, r_2)$.

Separation given by Equation 10 allows a direct calculation of the angular integrals. The radial ones are coupled through the two-dimensional terms $\tilde{U}_l(r_1, r_2)$. We numerically evaluate $\tilde{U}_l(r_1, r_2)$ by means of Equation 11 by performing a one dimensional integral at each point (r_1, r_2) belonging to a two dimensional grid of quadrature points. The radial partial-wave potentials can be stored in binary format on solid state memories for a fast access.

Let us now analyze how the relative coordinates r_1 , r_2 , and r_{12} can be associated to our particular physical system. There are two different ways to do this: by setting r_{12} as the H–H or by considering it to be one of the Li–H interparticle coordinates. Each choice will have a different partial wave treatment for U and a different convergence rate of the partial wave expansion given by Equation 4. Also, since $U^{(g)}$ is symmetric with respect to the interchange of the H atoms, we can take advantage of the corresponding parity of the wave function, which would reduce the effective size of the expansions by evaluating odd and even functions separately. If ones uses the asymmetric set, however, the two body asymptotic H–H interaction can be completely removed through one of the Equation 6. Since for this particular case the H–H interaction is stronger than the Li–H one, convergence of the asymmetric expansion would be faster in this sense.

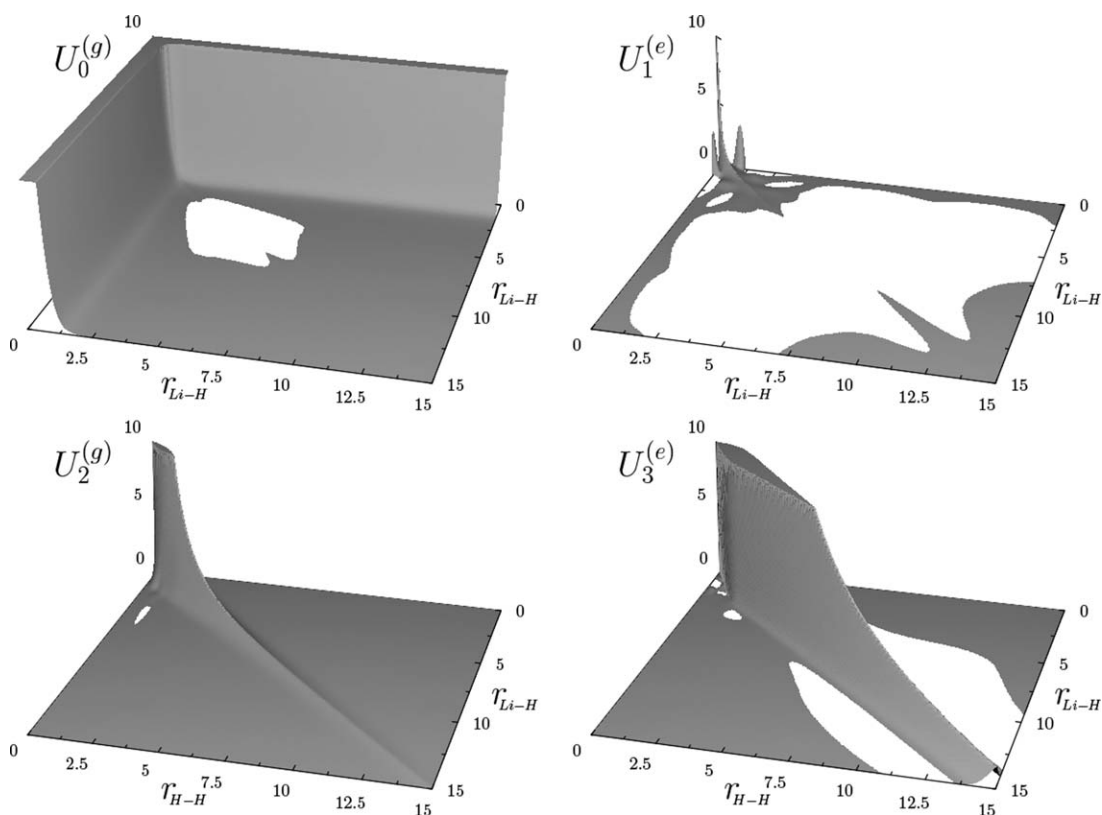


FIGURE 3 Three dimensional plots of the firsts partial-wave terms of the potentials $U_l^g(r_1, r_2)$ and $U_l^e(r_1, r_2)$, where r_1 and r_2 represent both Li—H (upper plots) and the H—H and Li—H (lower case) relative coordinates respectively, for different values of l . The domain of the plots in the z axis is $0 \leq z \leq 10$, and the white areas correspond to the region where the potential is attractive

In Figure 3, we show three-dimensional plots of the partial-wave decomposition of the potentials functions U_l^g and U_l^e when r_{12} corresponds to one of the H—H interparticle distance (upper panel) and to one of the Li—H ones (lower panel), for different values of l .

2.2 | Mass-scaled Jacobi coordinates

Jacobi coordinates for a three body system are defined as: $\mathbf{x} = \mathbf{r}_{12}$ and $\mathbf{X} = \frac{m_1 \mathbf{r}_1 + m_2 \mathbf{r}_2}{m_1 + m_2} - \mathbf{r}_3$, where \mathbf{X} is the relative position between one of the particles and the center of mass of the other two, whose relative position is \mathbf{x} . The advantage of these coordinates is that they lead to a diagonal form of the kinetic energy operator.^[18] The mass-scaled Jacobi coordinates (MSJC) \mathbf{R} and \mathbf{r} are defined by introducing scaling factors: $\mathbf{R} = (\mu_{3,12}/\mu_{12})^{1/4} \mathbf{X}$ and $\mathbf{r} = (\mu_{12}/\mu_{3,12})^{1/4} \mathbf{x}$, where $\mu_{3,12}$ is the reduced mass between the particle 3 and the other two. Using a three particle reduced mass $\mu = \left(\frac{m_1 m_2 m_3}{m_1 + m_2 + m_3}\right)^{1/2}$ we can do a further simplification of the kinetic energy operator, leaving the Schrodinger equation as:

$$\left[-\frac{1}{2\mu} (\nabla_{\mathbf{R}}^2 + \nabla_{\mathbf{r}}^2) + U(\mathbf{R}, \mathbf{r}, \theta_R) - E \right] \Psi(\mathbf{R}, \mathbf{r}) = 0. \tag{12}$$

The matrix representation of the hamiltonian is done in a similar way as for the RC case, where the GSF equations are now written as:

$$\left[-\frac{1}{2\mu} \frac{d^2}{dr^2} + U_r(r) - E_r + \beta_{n_r} V_r(r) \right] S_{n_r}(r) = 0 \tag{13}$$

and

$$\left[-\frac{1}{2\mu} \frac{d^2}{dR^2} + U_R(R) - E_R + \beta_{n_R} V_R(R) \right] S_{n_R}(R) = 0, \tag{14}$$

where U_r and U_R are:

$$U_r(r) = \text{Min}[U^{(j)}(R, r, \theta_R)] \{0 \leq R \leq \infty; 0 \leq \theta_R \leq \pi\} \tag{15}$$

and

$$U_R(R) = \text{Min}[U^{(j)}(R, r, \theta_R)] \{0 \leq r \leq \infty; 0 \leq \theta_R \leq \pi\} \tag{16}$$

The three-body basis elements are:

$$\Phi_{\nu}^{L,M}(\mathbf{R}, \mathbf{r}) = \frac{S_{n_R}(R) S_r(r)}{R r} \mathcal{Y}_{l_R, l_r}^{L,M}(\hat{\mathbf{R}}, \hat{\mathbf{r}}), \quad (17)$$

where $\nu = \{n_r, n_R, l_r, l_R\}$. The Galerkin method leads to a system equivalent to the given in Equation 8, but the matrix hamiltonian now reads: $\mathbf{H} = \mathbf{h}_r + \mathbf{h}_R + \mathbf{U}$, with:

$$\begin{aligned} [\mathbf{U}]_{\nu, \nu} &= \langle \Phi_{\nu}^{L,M} | \hat{U}(R, r, \cos \theta_{Rr}) | \Phi_{\nu}^{L,M} \rangle, \\ [\mathbf{O}_{\nu, \nu}] &= \langle \Phi_{\nu}^{L,M} | \Phi_{\nu}^{L,M} \rangle \\ [\mathbf{h}_r]_{\nu, \nu} &= \langle \Phi_{\nu}^{L,M} | -\beta_{n_r} V(r) + \frac{l_r(l_r + 1)}{2\mu r^2} | \Phi_{\nu}^{L,M} \rangle \end{aligned}$$

and

$$[\mathbf{h}_R]_{\nu, \nu} = \langle \Phi_{\nu}^{L,M} | -\beta_{n_R} V(r_R) + \frac{l_R(l_R + 1)}{2\mu R^2} | \Phi_{\nu}^{L,M} \rangle,$$

where $\hat{U}(R, r, \cos \theta_{Rr}) = U(R, r, \cos \theta_{Rr}) - U_R(R) - U_r(r)$ and $\hat{E} = E - E_R - E_r$. The three body potential \hat{U} it is written in a similar way as the RC basis:

$$\hat{U}(R, r, \cos \theta_{Rr}) = \sum_{l=0}^{\infty} \hat{U}_l(R, r) P_l(\cos \theta_{Rr}) \quad (18)$$

where:

$$\hat{U}_l(R, r) = \frac{2l+1}{2} \int_{-1}^1 \hat{u}(R, r, x) P_l(x) dx. \quad (19)$$

and $\hat{u}(R, r, x) = \hat{U}(R, r, (R^2 + r^2 - Rx)^{1/2})$. Figure 4 shows three dimensional plots of the partial-wave terms of the potentials U^{β} and U^e , respectively, as a function of r and R , when r represents the H—H or the Li—H distance for different values of l . Note that odd partial-wave terms are null for the symmetric MSCJ representation of U^{β} .

2.3 | Solution of the linear system

Equations 3 and 12 are mathematically identical, and their exact solutions must be the same. Numerical solutions, however, can present differences. Since we only use two vectors to describe the three-body dynamics, we can only include two of the three asymptotic interactions through the Sturmian RC Equation 6, while with the MSJC we can only include one of them (the corresponding to the r distance), through Equation 13. The remaining part of the potential \tilde{U} is decomposed through the partial wave series. The inclusion of the asymptotic potentials to the basis exactly matches the asymptotic two-body binding energies and states, and the convergence is accelerated respect to the use of other sets. We can then expect a difference in convergence between the RC and MSJC basis, because of the difference in the number of asymptotic interactions included in the basis.

Another difference we have to note between the use of RC and MSJC coordinates is the structure of the kinetic energy operator. Both expressions have almost the same form, except that the RC case includes an additional term (third term of Equation 3) which couples the coordinates. It has to be noted that for three-body systems where m_3 is much larger than m_1 and m_2 (such as in two-electron atomic systems), this term can be dismissed. Since in our method the Laplacian terms are removed through the basis equation, we see that the MSJC kinetic energy is to be exactly removed while with the RC basis it is not. Still the remaining matrix element (given in Equation 9) is separable and the angular integrals can be performed exactly. The disadvantage in this aspect resides in the fact that matrix elements (9) involve a complicated algebra which couples the angular momenta, and results in some loss of convergence rate of the RC expansion over the MSJC one (or over the $m_3 = \infty$ case).

For a given Hamiltonian structure given by the RC or MSJC representations, we still have to assign the particles to the reference system. We can choose between two different sets in both cases, which would allow us to quantify the advantages of the symmetric expansions over the asymmetric ones. In the RC treatment the symmetric expansion is obtained if we consider $r_1 = r_{Li-H(a)}$ and $r_2 = r_{Li-H(b)}$, where the suffixes a and b are introduced to distinguish between the two identical H atoms, while the asymmetric treatment is obtained with $r_1 = r_{Li-H(a)}$ and $r_2 = r_{H-H}$. For the MSJC the symmetric expansion corresponds to $r = r_{H-H}$ and $R = r_{Li-H_2}$ while the asymmetric one to $r = r_{Li-H}$ and $R = r_{H-LiH}$. Because of the symmetry of the interaction U^{β} , the partial wave terms given by Equations 11 and 19 are null for odd values of l .

In all cases, the potential energy surfaces depend on the three inter-particle coordinates, which means that the Hamiltonian commutes with the total angular momentum operator,^[16] and the solutions for each pair of L and M can be considered independently.

For all the vector coordinates employed, the linear system of equations becomes a generalized eigenvalue problem for \hat{E} with the structure given by Equation 8. The size of the system is defined as the size of the two dimensional radial basis ($N_1 \times N_2$ or $N_r \times N_R$) multiplied by the number of single pairs (l_1, l_2) or (l_r, l_R) included in the expansion, which are selected according to the triangle rule with the total angular momentum quantum

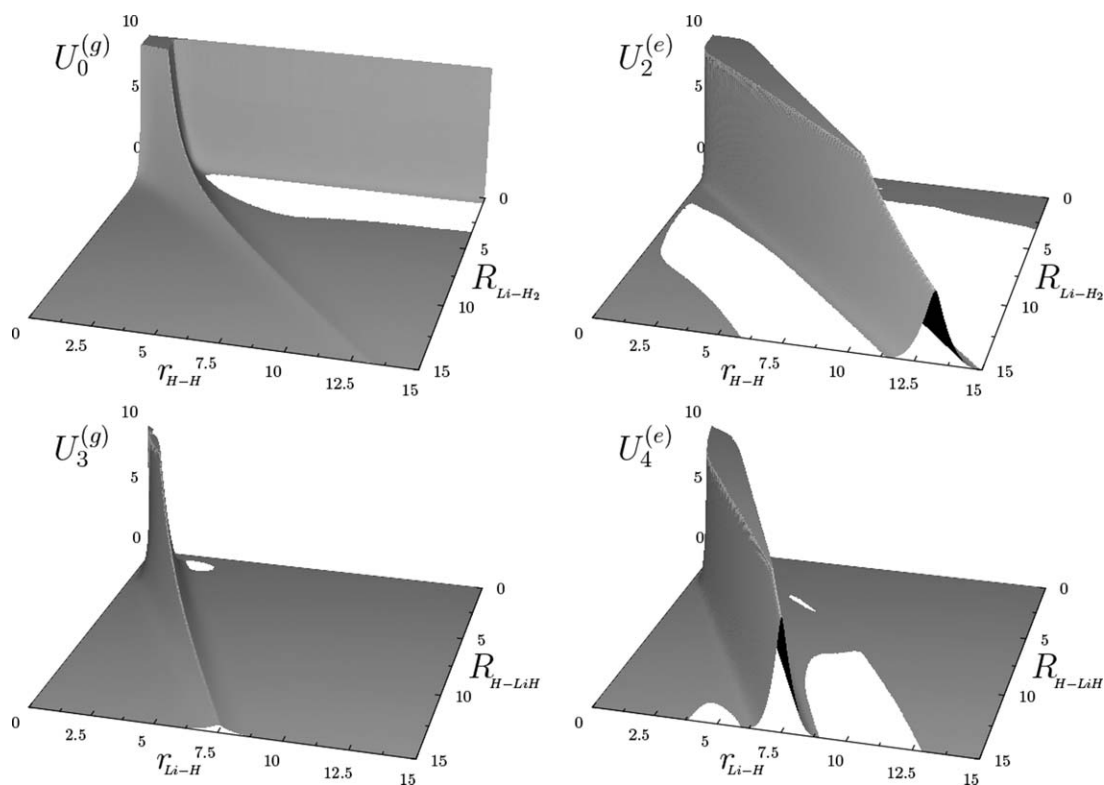


FIGURE 4 Three dimensional plots of the first partial wave terms of the potential $U_l^g(r, R)$ and $U_l^e(r, R)$, where r and R are the mass scaled Jacobi coordinates associated to the H—H and Li—H₂ (upper plots) and Li—H and H—LiH coordinates (lower case) respectively, for different values of l . The domain of the plots in the z axis is $0 \leq z \leq 10$, the white areas correspond to regions where the potential is attractive

number L . The overlap matrix \mathbf{O} is first inverted, and then the solution to the eigen-system defined by the matrix $\mathbf{O}^{-1}\mathbf{H}$ is obtained, all the algebraic operations performed with lapack.^[19] Convergence for each case is studied in next section.

2.4 | Sudden electronic transition

Once evaluation of the three-body has been performed, the dynamics under a sudden change of the PES can be considered. This abrupt change in the potential can be actually produced by an electronic transition, since the electronic movement is assumed to be much faster than that of the nuclei, and the molecular states have not time to evolve while the electronic transition occurs.

If $|\Psi_n^e\rangle$ is the n th eigenstate of the hamiltonian corresponding to the potential U^e and $|\Psi_n^g\rangle$ those corresponding to U^g , we can write:

$$|\Psi_n^e\rangle = \sum_m c_{n,m}^{(g \rightarrow e)} |\Psi_m^g\rangle, \tag{20}$$

where

$$c_{n,m}^{(g \rightarrow e)} = \langle \Psi_m^g | \Psi_n^e \rangle \tag{21}$$

since the eigenstates conform a complete ortho-normal set. After a sudden transition, the eigenstate $|\Psi_n^e\rangle$ is going to evolve in time according to:

$$|\Psi(t)\rangle = \sum_m c_{n,m}^{(g \rightarrow e)} e^{-iE_m^g t} |\Psi_m^g\rangle \tag{22}$$

where E_m^g are the eigen-energies associated to H^g . An example of such a sudden electronic transition will be briefly analyzed through a practical calculation in the next section.

3 | RESULTS AND DISCUSSION

Let us now test the convergence of the method, both, as a function of the number of radial orbitals and as the number of partial-waves included. The system of Equations 8 has a block structure, each block corresponding to two pairs of orbital angular momentum quantum numbers (l_1, l_2) or (l_r, l_i) , and a where the size of each block correspond to the number radial functions $N_1 \times N_2$ or $N_r \times N_i$ (one for each radial coordinate). The system can be viewed as system of two dimensional differential radial equations, coupled through \hat{U} and the matrix element (9) in the RC case.

TABLE 1 Convergence of the s-wave ground state energy of the LiH_2^+ system in the ground state PES as a function of the number of radial basis functions for the two different RC systems

N_{\max}	s-Wave ground state energy of U^{β}	
	RC	
	$(r_{\text{Li-H}}, r_{\text{Li-H}})$	$(r_{\text{Li-H}}, r_{\text{H-H}})$
5	-0.024 833 215	-0.168 900 569
10	-0.024 949 046	-0.168 900 766
15	-0.025 006 992	-0.168 900 775
20	-0.025 024 609	-0.168 900 799
25	-0.025 027 406	-0.168 900 804
30	-0.025 027 973	-0.168 900 804
35	-0.025 028 305	-0.168 900 804

By setting $L=M=0$, and only one pair of two-particle angular momentum quantum numbers, the system reduces to only one two-dimensional radial equation. Convergence rate of the solutions of this simple system depends on the size of the radial domain considered, and the characteristics of the basis set. There are infinitely many ways to define Sturmian Functions, both through the functional space of the generating potentials V at the Sturmian equation, or by changing the externally defined energy of the basis, as described in Ref. [12].

Since we are dealing with several coordinate systems and we define a particular set for each case, we simplify the task by choosing the same generating potential V in Equations 6, 14, and 13 to be a constant, turning the basis set into a energy eigenfunctions. We have checked that a Yukawa potential can improve the radial convergence, being however the exponential parameter different for each coordinate system. The energy of the Sturmian equations is chosen to be -0.5 a. u. for the coordinates related to the H–H dynamics and -0.004 in $r_{\text{Li-H}}$, $R_{\text{Li-HH}}$ or $R_{\text{H-LiH}}$, which are close to the energies of the two body systems H–H and Li–H. This values simulate approximately the fall of behavior as the particles move away from each other^[12] when using the Yukawa potential.

It has to be taken into account that variations in convergence between choosing the optimal (variational) energy or potential and one approximated, can be easily compensated by adding some radial functions. The exact values employed in this calculation are introduced for reproducibility purposes. The radial integrals were performed with 120 points Legendre–Gauss quadrature, which stabilizes the energy in the seventh significant figures.

The results presented here correspond to the surfaces U^{β} and U^{ϵ} , and we explore all possible configurations both for the RC and MSJC coordinates in the symmetrical and asymmetrical cases. This makes a total of 8 different approaches to the same differential equation.

Convergence of the s-wave ground state energy associated to the potential U^{β} as a function of the maximum number of radial orbitals per radial coordinate N_{\max} is shown in Tables 1 and 2, where we see that the converged values are different for each coordinate configuration. This is because the s-wave equation is different in each case. In Figure 1 we can observe the magnitudes of U at the asymptotic two-body regions, where we see that for U^{β} the H–H interaction is deeper than the Li–H one.

By using $r_{\text{H-H}}$ either in the RC or MSJC coordinates, the potential would be implicitly considered in the expansion through the Sturmian equation, while in the other cases it would be approximated through the partial wave series. This is why cases $(r_{\text{Li-H}}, r_{\text{H-H}})$ and $(r_{\text{H-H}}, R_{\text{Li-HH}})$ gives a deeper value of the energy than $(r_{\text{Li-H}}^{(a)}, r_{\text{Li-H}}^{(b)})$ and $(r_{\text{Li-H}}, R_{\text{H-LiH}})$. The small differences between the energies of these two groups depend on the details of the potentials.

TABLE 2 Same as Table 1, but for the different MSJC coordinate systems

N_{\max}	s-Wave ground state energy of U^{β}	
	MSJC	
	$(r_{\text{Li-H}}, R_{\text{H-LiH}})$	$(r_{\text{H-H}}, R_{\text{Li-HH}})$
5	-0.026 894 411	-0.170 558 872
10	-0.041 690 634	-0.170 558 948
15	-0.048 919 739	-0.170 559 011
20	-0.052 994 324	-0.170 559 019
25	-0.055 802 555	-0.170 559 021
30	-0.057 942 825	-0.170 559 025
35	-0.059 572 098	-0.170 559 030

TABLE 3 Convergence of the ground state energy of the LiH_2^+ triatomic system under the U^β potential, as a function of the maximum number of partial waves included for each coordinate, when the number of radial basis functions per coordinate is 20

L_{\max}	Partial-wave expansion of the ground state energy of U^β	
	RC	
	$(r_{\text{Li-H}}, r_{\text{Li-H}})$	$(r_{\text{H-H}}, r_{\text{Li-H}})$
0	-0.025 024 608	-0.169 531 909
1	-0.070 359 173	-0.170 016 841
2	-0.104 845 153	-0.171 567 034
3	-0.125 984 531	-0.171 906 083
4	-0.138 569 732	-0.172 180 927
5	-0.146 554 248	-0.172 320 240
6	-0.151 796 444	-0.172 368 895
7	-0.155 232 537	-0.172 393 243
8	-0.157 540 328	-0.172 401 695
9	-0.159 146 002	-0.172 404 466
10	-0.160 333 182	-0.172 405 375
11	-0.161 320 047	-0.172 405 653
12	-0.162 260 077	-0.172 405 721

The differences in the final values indicate the efficiency of the different RC coordinates.

We use results shown in Tables 1 and 2 to determine an acceptable value of the radial basis size. We chose $N_{\max} = 20$, which gives convergence between the fourth and sixth significant figure, and assume that this value would give also good results for the U^e eigenstates. The next step is to check convergence of the energies as increasing the maximum number of partial waves included in the basis. $L = 0$ results for the ground state corresponding to the PES U^β in the RC and MSJC are given in Tables 3 and 4, while those corresponding to U^e are shown in Tables 5 and 6 respectively.

TABLE 4 Same as Table 3, but for the MSJC coordinates

L_{\max}	Partial-wave expansion of the ground state energy of U^β	
	MSJC	
	$(r_{\text{Li-H}}, R_{\text{H-LiH}})$	$(r_{\text{H-H}}, R_{\text{Li-H}_2})$
0	-0.052 994 324	-0.170 559 020
1	-0.131 949 219	-0.170 559 020
2	-0.153 958 139	-0.172 173 000
3	-0.160 950 531	-0.172 173 000
4	-0.163 849 911	-0.172 416 308
5	-0.165 274 362	-0.172 416 308
6	-0.166 146 281	-0.172 434 765
7	-0.166 836 275	-0.172 434 765
8	-0.167 581 411	-0.172 435 423
9	-0.168 998 573	-0.172 435 423
10	-0.170 246 487	-0.172 435 436
11	-0.170 986 319	-0.172 435 436
12	-0.171 667 983	-0.172 435 436

TABLE 5 Same as Table 3, but for the U^e potential

L_{\max}	Partial-wave expansion of the ground state energy of U^e	
	RC	
	(r_{Li-H}, r_{Li-H})	(r_{H-H}, r_{Li-H})
0	-0.115 582 147	-0.112 178 178
1	-0.115 582 147	-0.124 729 688
2	-0.125 050 714	-0.131 077 452
3	-0.129 326 005	-0.133 132 011
4	-0.131 540 451	-0.133 924 687
5	-0.132 779 921	-0.134 233 345
6	-0.133 500 935	-0.134 338 745
7	-0.133 926 973	-0.134 364 604
8	-0.134 177 609	-0.134 367 787
9	-0.134 321 330	-0.134 367 809
10	-0.134 399 905	-0.134 367 920
11	-0.134 440 019	-0.134 368 012
12	-0.134 458 867	-0.134 368 035

Results are shown as a function of L_{\max} , the parameter which approximates the potential. Triangle selection rule for the $L = 0$ angular integrals imply that the two particle orbital angular momentum pairs are equal $l_1 = l_2$, and that they can run from 0 to $2L_{\max}$. The size of each linear system is thus $N_{\max}^2 \times (2L_{\max} + 1)$.

We can see that for U^{β} the best convergence rate is obtained with the symmetric MSJC and asymmetric RC systems, because of the way the potentials are included in the basis. If the H-H interaction is treated through the partial wave series, again the MSCJ (asymmetric) gives better results than the RC (symmetric). A different result is obtained for U^e , where the deepest energy value is obtained with the asymmetric MSJC which

TABLE 6 Same as Table 4, but for the U^e potential

L_{\max}	Partial-wave expansion of the ground state energy of U^e	
	MSJC	
	(r_{Li-H}, R_{H-LiH})	(r_{H-H}, R_{Li-H_2})
0	-0.109 632 969	-0.113 471 260
1	-0.120 887 130	-0.117 040 961
2	-0.128 782 356	-0.125 425 455
3	-0.131 861 851	-0.129 428 056
4	-0.133 309 331	-0.129 428 056
5	-0.134 046 448	-0.132 739 449
6	-0.134 433 810	-0.133 450 023
7	-0.134 635 534	-0.133 879 706
8	-0.134 735 277	-0.134 138 124
9	-0.134 779 999	-0.134 291 253
10	-0.134 797 354	-0.134 378 315
11	-0.134 802 968	-0.134 425 244
12	-0.134 804 485	-0.134 448 793

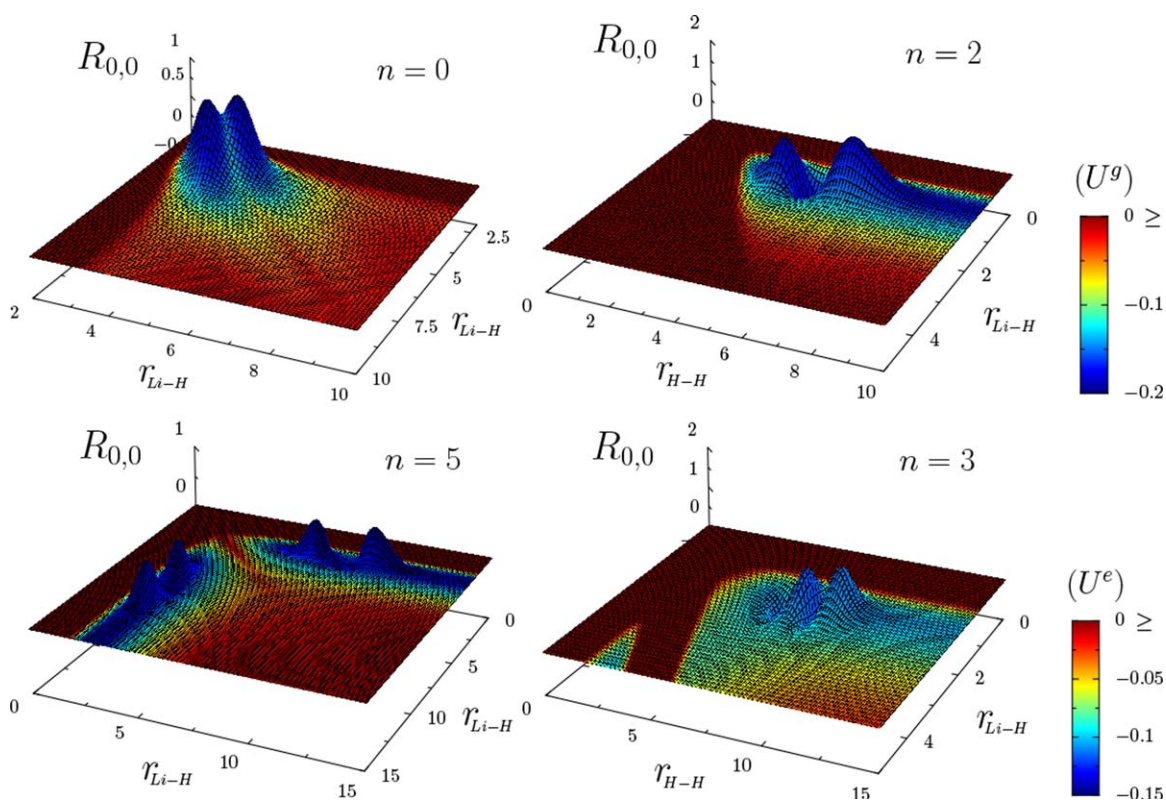


FIGURE 5 Three dimensional plots of the radial partial-wave components of the ground and some excited states, as a function of the different sets of relative coordinates, for the ground and first excited electronic state PES. Through the color superimposed on the surface indicates the value of the first partial-wave component of the potential of the corresponding coordinate set

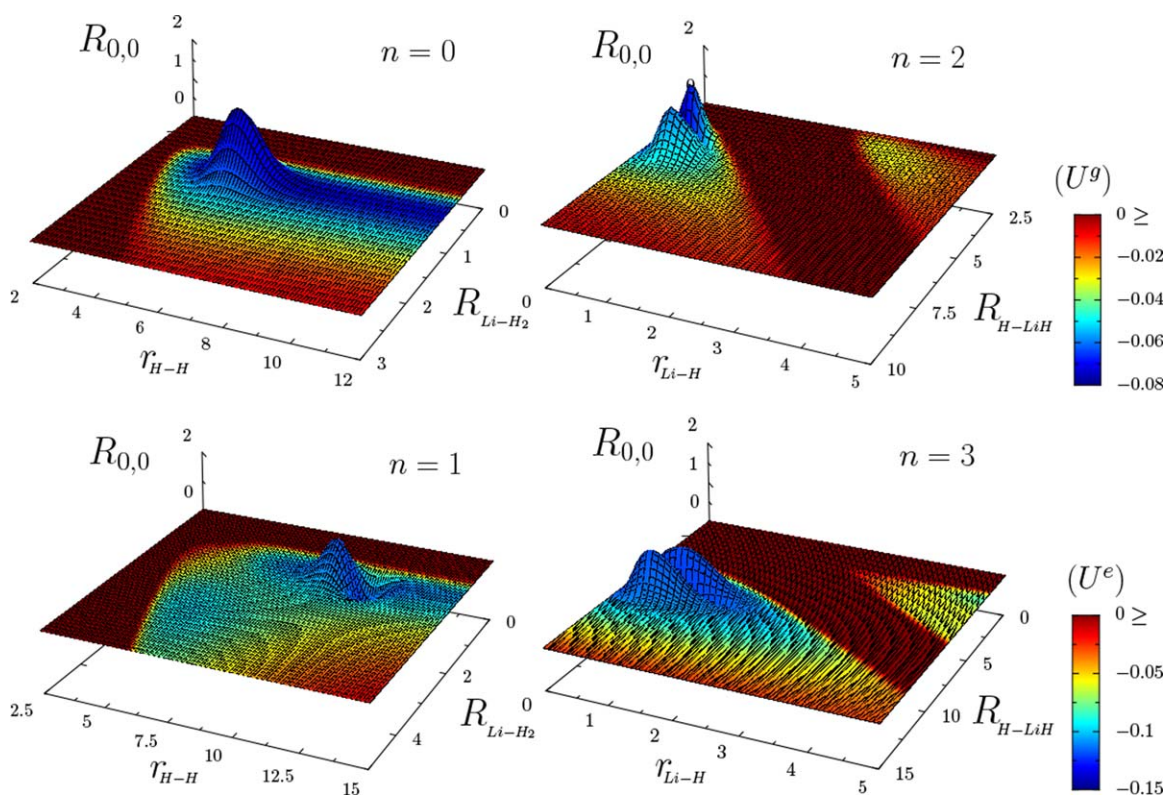


FIGURE 6 Same as Figure 5, in this case for the mass scaled Jacobi coordinates

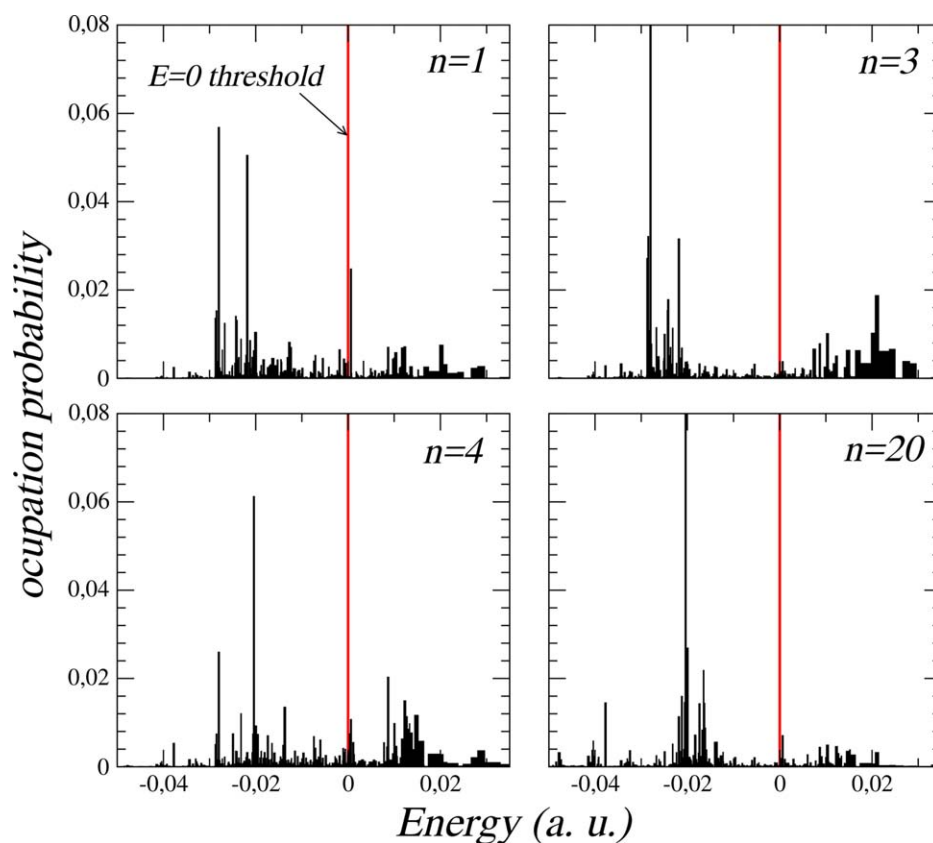


FIGURE 7 Occupation coefficients of the ground state associated to the ground electronic PES, as a function of the energies of the occupied final eigenstates corresponding to the first excited PES

explicitly employs the r_{U-H} coordinate, followed by the symmetric MSJC. For the RC case, the symmetric system shows better results than the asymmetric one. In this case the asymptotic two-body interactions are of the same order of magnitude and we cannot say a priori why one system gives better convergence than the other. This shows that the advantages in the convergence rate of one system respect to another strongly depends on the particular physical system.

The first partial-wave radial functions corresponding to some bound states corresponding to the ground (U^g) and first excited (U^e) PES, as a function of the RC and MSJC radial coordinates, are shown in Figures 5 and 6, respectively. The surfaces are colored according to the value of the first radial partial wave potential for the same coordinate values. We can see that the eigenstates concentrate at the minimum of the potential. For each eigenstate, the higher partial-wave radial functions (not shown) nodal structure and radial distribution.

Let us now consider the situation described in the above section, where a sudden change in the three body interatomic potential occurs. In expressions given by Equations 20–22, we considered discrete sums, as if the whole spectrum of the hamiltonian were discrete. Being rigorous, there are also continuum wave functions, which in our case become approximated by square-integrable pseudo states. If the discretization of these continuum levels is dense enough there will be an accurate description to the continuum. Those coefficients given by (21) which are different from zero, and which correspond to $E_m^g > 0$ will give us a measure of the fragmentation probability.

In Figure 7, we show the square of the expansion coefficients given by Equation 21 for $n = 1, 3, 4,$ and 20 of the ground state associated to the potential U^e as a function of the eigenstates energies of U^g . The result corresponds to an energy probability distribution, corresponding to the possible final states, showing finite values for positive energies, which are associated to the fragmentation of the system into two and three body fragments.

4 | CONCLUSIONS

In this work, we deal with the three body LiH_2^+ molecular system in the Born–Oppenheimer approximation, where the potential energy surfaces PES defined by the ground and first excited electronic levels were used to describe the nuclear dynamics. The potential energy surfaces were the ones obtained by Martinazzo et al. by means of a multireference valence bond approach within a spin-coupled formulation.^[7]

The atomic dynamics was studied under the quantum regime, solving the three body Schrödinger equation for the two PES's in the following different coordinate systems: (a) a pair of relative coordinate vectors and (b) a mass scaled Jacobi coordinate pairs. The eigenstates of the hamiltonian and eigenfunctions of the total angular momentum operator and projection over a given axes were expressed in terms of Generalized Sturmian

Functions, composed by a set of bispherical harmonics for the angular dynamics, and a pair of Sturmian functions for the radial ones. The radial Sturmians were defined according to the coordinate they were assigned to represent. In each case, we introduced a potential that for a given value of the coordinate, it correspond to the minimum value of potential in the remaining part of the configuration space. This allowed us to include part of the three body dynamics both, through the relative coordinates and through the Jacobi coordinate related to the distance of one of the particles with the center of mass of the other two.

The remaining part of the potential was introduced through a partial wave decomposition in a two dimensional quadrature grid, where we evaluate the projection over Legendre polynomials. This procedure is the typical decomposition made with the Coulomb potential in atomic calculations. The procedure was done and tested over the different sets, and for both PES's.

Evaluation of the radial convergence was done with an s-wave approach, to determine an optimal radial basis. Then, the partial-wave convergence was performed both for the ground and excited state PES, in the RC and MSJC, in their symmetric and asymmetric implementations, making a total of eight approaches to the same equation.

We presented a brief example of application by considering the dynamics of the ground state of the excited state PES after a sudden transition of the electronic state to the ground state, abruptly modifying the three atomic potentials. As a result, population of the states of the ground state PES (those which preserve symmetry) occurred, with the probability of the whole system breaking up partially or totally.

The present work aim is to introduce the generalized Sturmian method as a useful tool for molecular calculation and reactive dynamics.

ACKNOWLEDGMENTS

We acknowledge the Universidad Nacional de Cuyo (project No. 06/C480), FONCYT (PICT-2014-1400) and CONICET for funding. The authors also like to thanks to professor R. Martinazzo and collaborators for providing the PES software.

ORCID

Juan M. Randazzo  <http://orcid.org/0000-0002-1849-899X>

REFERENCES

- [1] S. Bovino, T. Stoecklin, F. A. Gianturco, *Astrophys. J.* **2010**, *708*, 1560.
- [2] S. Bovino, M. Tacconi, F. A. Gianturco, T. Stoecklin, *Astrophys. J.* **2010**, *724*, 126.
- [3] S. Bovino, M. Tacconi, F. A. Gianturco, D. Galli, F. Palla, *Astrophys. J.* **2011**, *731*, 107.
- [4] E. Bodo, F. A. Gianturco, R. Martinazzo, M. Raimondi, *Chem. Phys.* **2001**, *271*, 309.
- [5] S. Lepp, P. C. Stancil, A. Dalgarno, *J. Phys. B At. Mol. Opt. Phys.* **2002**, *35*, R57.
- [6] R. Martinazzo, G. F. Tantarini, E. Bodo, F. A. Gianturco, *J. Chem. Phys.* **2003**, *119*, 11241.
- [7] R. Martinazzo, E. Bodo, F. Gianturco, M. Raimondi, *Chem. Phys.* **2003**, *287*, 335.
- [8] E. Bodo, F. A. Gianturco, R. Martinazzo, A. Forni, M. Raimondi, *J. Phys. Chem. A* **2000**, *104*, 11972.
- [9] R. Martinazzo, A. Famulari, M. Raimondi, E. Bodo, F. A. Gianturco, *J. Chem. Phys.* **2001**, *115*, 2917.
- [10] D. A. McCormack, G.-J. Kroes, *Chem. Phys. Lett.* **2002**, *352*, 281.
- [11] G. Gasaneo, L. U. Ancarani, D. M. Mitnik, J. M. Randazzo, A. L. Frapiccini, F. D. Colavecchia, *Adv. Quantum Chem.* **2013**, *67*, 153.
- [12] J. M. Randazzo, L. U. Ancarani, G. Gasaneo, A. L. Frapiccini, F. D. Colavecchia, *Phys. Rev. A* **2010**, *81*, 042520.
- [13] J. M. Randazzo, D. Mitnik, G. Gasaneo, L. U. Ancarani, F. D. Colavecchia, *Eur. Phys. J. D* **2015**, *69*, 189.
- [14] M. Ambrosio, D. M. Mitnik, G. Gasaneo, J. M. Randazzo, A. S. Kadyrov, D. V. Fursa, I. Bray, *Phys. Rev. A* **2015**, *92*, 052518.
- [15] J. M. Randazzo, C. A. Rios, *J. Phys. B At. Mol. Opt. Phys.* **2016**, *49*, 235003.
- [16] C. Cohen-Tannoudji, B. Diu, F. Laloe, *Quantum Mechanics*, Vol. 1, Wiley, New York **1991**.
- [17] D. M. Mitnik, F. D. Colavecchia, G. Gasaneo, J. M. Randazzo, *Comput. Phys. Commun.* **2011**, *182*, 1145.
- [18] J. M. Bowman, J. Ziga, A. Wierzbicki, *J. Chem. Phys.* **1989**, *90*, 2708.
- [19] E. Anderson, Z. Bai, C. Bischof, S. Blackford, J. Demmel, J. Dongarra, J. Du Croz, A. Greenbaum, S. Hammarling, A. McKenney, D. Sorensen, *LAPACK Users' Guide*, 3rd ed., Society for Industrial and Applied Mathematics, Philadelphia, PA **1999**.

How to cite this article: Randazzo JM, Aguilar-Navarro A. Three-body molecular states of the LiH_2^+ system in the Born–Oppenheimer approximation. *Int J Quantum Chem.* 2018;e25611. <https://doi.org/10.1002/qua.25611>